

Synthesis and Characterization of LaFeO₃ nanoparticles at low temperature

P. S. R. Murthy, Ciano Fernandes, Shubham Gaonkar, Samruddhi Azrekar, Apoorba Singh

^aDhempe College of Arts and Science, Goa, India.

ABSTRACT:

The synthesis, structure and characterization of LaFeO₃ nanoparticles were studied using a simple sol-gel combustion method. The overall process involves three steps – formation of homogenous solution, formation of dried gel and final combustion of the dried gel. On ignition in air, the compound is found to transform into nanosized LaFeO₃ nanoparticles. The analysis of X-ray diffraction (XRD) data confirmed the orthorhombic LaNiO₃ perovskite of space group *Pnma* without any impurity phase. The Scherrer's formula was employed to estimate the crystallite size of the prepared sample. For a further insight into the crystal structure, Scanning electron microscopy (SEM) imaging was done. The estimated values of the crystallite size from Scherrer's formula and SEM were found to be roughly the same. The SEM images confirmed the polycrystalline nature of the prepared sample. Furthermore, UV measurements were performed on the compound to estimate its band gap energy. The values were found to match well with those reported elsewhere in literature. EDX measurements performed on the sample confirmed the existence of La, Fe and O elements.

KEYWORDS: Auto-combustion, Rietveld refinement, nanoparticles, orthorhombic, diffuse reflectance.

Date of Submission: 10-07-2020

Date of acceptance: 26-07-2020

I. INTRODUCTION

The LaFeO₃ perovskite herein referred to as LFO and related compounds have received considerable attention due to their wide uses in fuel cells [1], catalysts [2] and environmental monitoring applications [3]. The preparation of LFO and other related compounds have been achieved by many methods, including sol-gel [4,5], combustion synthesis [6-8] and hydrothermal synthesis [9]. However, all these wet chemical methods, to some extent, still require calcinations at relatively high temperature and long soaking to produce powders with good crystal structure. This leads to making the crystalline grains grow larger in size and weakens the reactivity, and hence obtaining nanosized particles is difficult. Hence, in LFO, we have followed a novel means to prepare monophasic nanosized LFO powder by the sol-gel process and low temperature combustion processes and do not require further clarification [10].

In LFO, the 3d electron configuration is known to contribute to magnetic ordering of the transition metal ions within the material. Among the large number of rare-earth perovskites, Lanthanum Orthoferrite (LFO) is known as a famous antiferromagnetic composition with a high Neel temperature (T_N - 740°C) and possesses a distorted perovskite structure with a *Pbnm* or *Pnma* space group due to the tilting of the octahedral [FeO₆]. This perovskite is also known to possess a high thermal stability and a well defined structure. All these interesting properties have resulted in this material being applied to a number of technological applications. In the present study, nano-synthesized LFO was prepared using a citrate-nitrate auto-combustion technique. In addition, characterization by X-ray diffraction that gives information about the crystal structure, crystal composition, lattice parameter, spacing between two crystal planes, particle size, FTIR (Fourier Transform Infrared Analysis) for knowing the molecular bonding between the atoms, UV-Visible spectroscopy that uses absorbance or reflectance in the visible region of the EM spectra to find the band gap energy in the sample, Scanning electron microscopy (SEM) to study the morphological structure and composition analysis of the sample and EDX to confirm composition of the sample elements were performed.

In the present study, nano-synthesized LFO was prepared using a citrate-nitrate auto combustion technique at room temperature. In addition to determining the particle size using different methods, the structure of the perovskite LFO was investigated using X-ray diffraction (XRD), the optical band gap energy of the compound was determined using UV-visible diffuse reflectance spectra and Energy dispersive X-ray measurements were performed to confirm the sample composition.

II. EXPERIMENTAL

LaFeO₃ was prepared using a citrate-nitrate auto-combustion method. Analytical grade La(NO₃)₂·6H₂O and Fe(NO₃)₂·9H₂O were used as starting materials. The metal nitrates were discretely dissolved in distilled water and then mixed together under constant stirring at 70°C. Citric acid was added to the mixture and the pH of the solution was controlled by drop-wise adding of proper amount of ammonia solution during the stirring process as so maintain the pH = 7. Ethylene glycol was then added to the mixture and heated at about 200°C in open air by decomposing the dried gel and finally a dark brown powder was formed after an intense exothermic combustion reaction. The powder was ground and then calcined at 600°C for three hours followed by pelletization and sintering at 600°C for five hours. Nanocrystalline LFO was obtained.

The sample was deemed to be phase pure, as X-ray diffraction recorded (XRD) data collected on a Rigaku X-ray diffractometer in the range of $10^\circ \leq \Theta \leq 80^\circ$ using CuK_α ($\lambda = 1.5418 \text{ \AA}$) radiation showed no impurity reflections. The diffraction patterns was Rietveld refined using FULLPROF suite and structural parameters were obtained. Fourier-transform infrared spectroscopy data was recorded for the sample in the range of 4000 cm⁻¹ to 500 cm⁻¹ at the Research centre of Dhempe College. UV-visible diffuse reflectance spectra were recorded for the sample in the range of 200 to 800 nm at the Department of Physics, Goa University. Scanning electron microscope (SEM) image and Energy dispersive X-ray spectrometer were recorded on the Zeiss make scanning electron microscope at the Instrumentation Centre, Goa University.

III. RESULTS AND DISCUSSION

Fig. 1 shows the room temperature Rietveld refined XRD pattern of the gel combustion synthesized LFO powder prepared by the citrate-nitrate auto-combustion technique. The XRD pattern confirms the formation of a pure LFO phase with a well-defined orthorhombic structure in the space group SG Pnma, without any impurity phase. The diffraction data are in good agreement with JCPDS card of LaFeO₃ (JCPDS no: 37-1493) [11]. The ideal cubic structure is not formed because of the distortion of the corner sharing octahedral due to the size mismatch of La³⁺ and Fe³⁺ [12], the parameter related to this being the tolerance factor ‘t’. Any deviation from $t = 1$ (ideal cubic structure), leads to a distorted structure such as orthorhombic, rhombohedral and tetragonal. The orthorhombic structure Pnma is a result of the FeO₆ octahedra tilting and rotation leading to a closer packing with the said structure. The tilt angle ϕ_{in} and ϕ_{out} as seen in Fig. 2 is related to the in-of-phase octahedral rotation around the [110] corresponding to the b-axis in the Pnma phase and ϕ_{out} octahedral rotation around the [001] corresponding to the c-axis in the Pnma phase [12, 13].

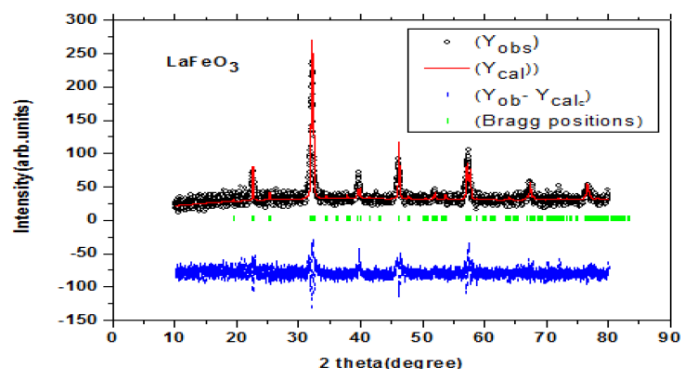


Fig.1. Rietveld refined XRD pattern for LFO. The open circles (black) show the observed counts, the continuous line (red) passing through these counts is the calculated profile, and the difference between the observed and calculated (blue) is shown as a common line at the bottom of the two profiles. The Bragg positions (green) are shown as vertical bars.

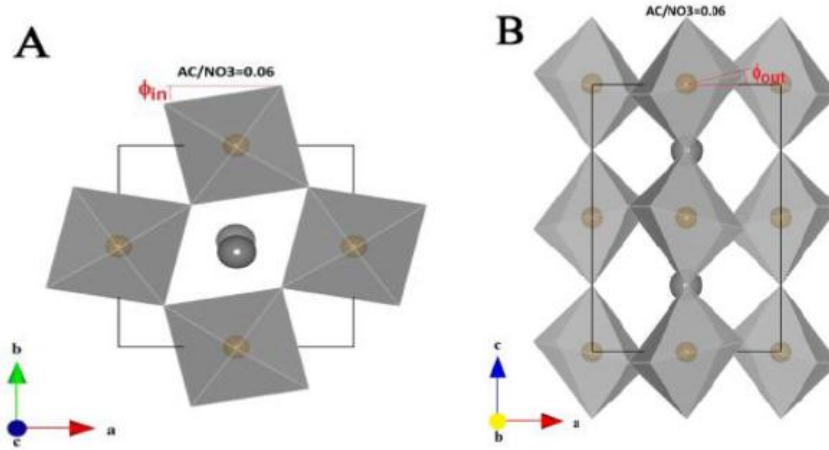


Fig.2. LFO A) along b axis for ϕ_{in} and B) along c axis for ϕ_{out} .

The FULLPROF program was used for Rietveld analysis of the XRD data of LFO as seen in Fig.2. Refinements were performed in the space group $Pnma$. In each refinement, a total of more than twenty parameters were refined: zero shift, scale factor, background coefficients, lattice parameters, oxygen parameters for isotropic temperature factor and full width at half maximum. The observed intensity data are plotted in the upper section as points (Black). The calculated intensities are shown in the same section as curves (Red). The difference between the observed and calculated intensities is shown in the lower section (Blue line). The short vertical bars in the centre of the plot show the Bragg positions (Green). Atomic coordinates for each cation in the A and B sites, the residual errors, and the refined lattice parameters for the orthorhombic LFO perovskite with the space group $Pnma$ are displayed in Table 1.

Label	Type	Atomic coordinates			Biso	Occupancy
		x	y	z		
La	La	0.02740	0.25	-0.00450	0.40000	0.44086
Fe	Fe	0	0	0.5	0.40000	0.55137
O1	O	0.25	0.25	0.075	1.16834	0.89000
O2	O	0.035	0.035	-0.27700	1.16834	0.11000

$$\alpha = \beta = \gamma = 90^\circ$$

$a/\text{Å}$	5.5177	R_{exp}	1.87
$b/\text{Å}$	7.8580	R_{wp}	4.76%
$c/\text{Å}$	5.5958	R_p	4.56%
$V/\text{Å}^3$	242.21	χ^2	1.21
a/b	0.7021	R-factor	1.65%
c/b	0.7121	RF-factor	1.26%

Table 1: Atomic coordinates for each cation in the A and B sites, R factors, equivalent thermal parameters and refined lattice parameters for the orthorhombic LFO perovskite with space group $Pnma$.

Fig. 3 indicates the crystalline size of the LFO sample calculated by using the X-ray line broadening method and the Scherrer's formula $D = k\lambda/\beta\cos\Theta$ where D is the crystallite size in nanometers, λ is the beam wavelength ($\lambda = 1.5414 \text{ \AA}$), k is a constant equal to 0.94, β is the integral breadth and Θ is the peak position. The average crystalline size is calculated to be about 33.7 nm. This is found to be in close agreement with that reported in literature elsewhere [10].

To understand the vibrational properties of the LFO nanoparticles, Fourier-transform infrared spectroscopy (FTIR) was performed on the sample in the range of 4000 cm^{-1} to 500 cm^{-1} as shown in Fig. 4. The peak at 2328 cm^{-1} is attributed to the strong O-H stretching vibration originating from condensed waters such as ambient water and incompletely reacted citric acid in our experiment. Two other absorption peaks at 718 and 957 cm^{-1} were also observed which are assigned to the Fe-O stretching and the bending vibration mode, respectively. These two peaks are a characteristic of the octahedral FeO_6 groups in the perovskite compound and reveal the existence of the LFO phase.

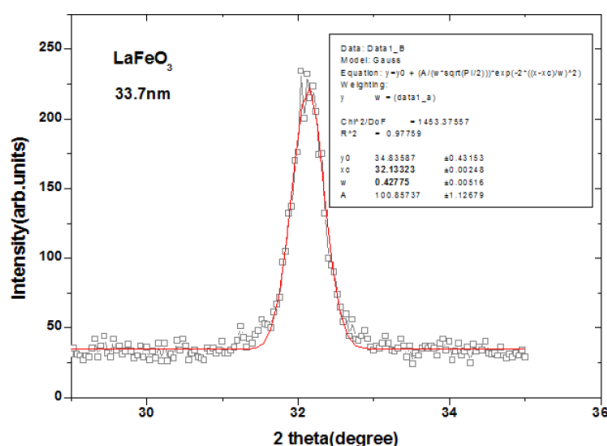


Fig. 3. Gaussian fit to the XRD data for determining particle size of LFO.

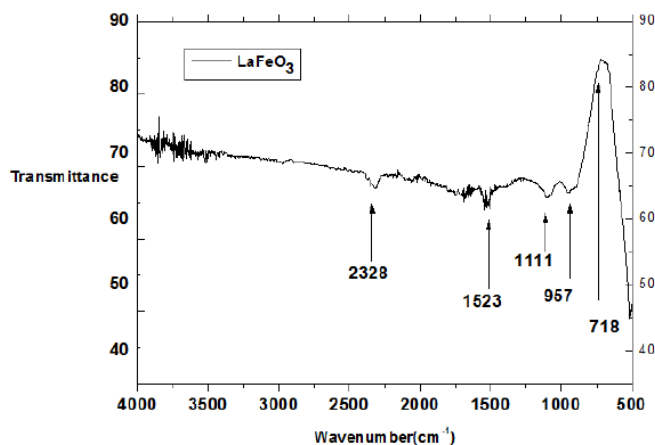


Fig. 4. FTIR for LFO in the range 4000 cm^{-1} to 500 cm^{-1} .

For semiconductor materials, the energy bandgap can be determined by their optical absorption performance. The UV visible diffuse reflectance spectra of the LFO nanoparticles in terms of absorbance as seen in Fig. 5 was collected as a function of the wavelength in nm. The optical bandgap of the LFO nanoparticles can be deduced from the spectra by determining the cut-off wavelength λ_c from the spectra. The bandgap of the LFO nanoparticles was determined to be 1.7 eV. This is much lower than that reported for the orthorhombic LFO of 2.45 eV [14].

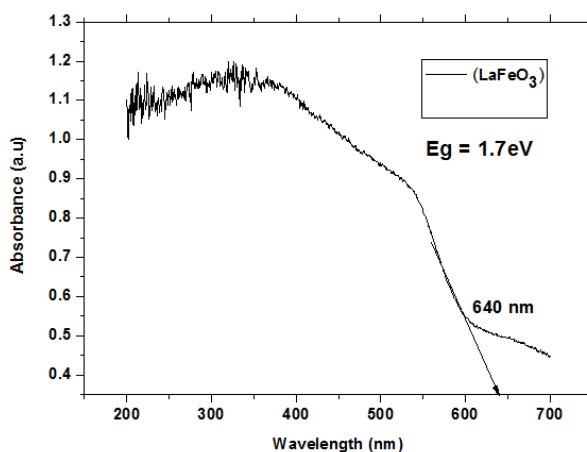


Fig. 5. UV spectra for LFO.

SEM was employed to obtain direct information about the size and structure of the produced LFO nanocrystals. Fig. 6 presents a typical SEM image that shows monodisperse particles with an average size of 31.2 nm, which is consistent with the size obtained from the peak broadening in X-ray diffraction studied of LFO. Such a consistency implies that the LFO nanoparticles are single crystalline.

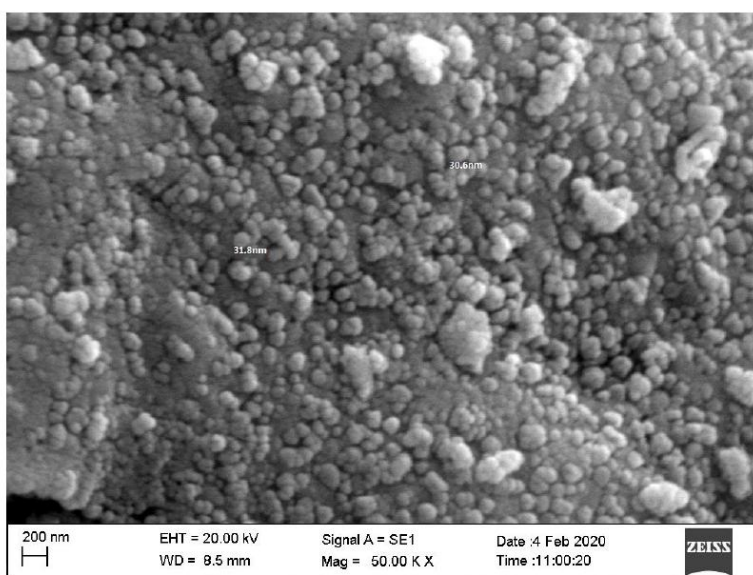


Fig. 6. SEM measurements for LFO with indication of particle size of 30.4 nm and 31.8 nm at 50K magnification.

Energy dispersive X-ray was performed on the LFO sample to confirm the sample composition. Three different areas of the sample were arbitrarily selected to ascertain the sample composition. The EDX results from the sample as seen in Fig. 7 confirm the existence of La, Fe and O elements. The elements present are La, Fe and O with a mole ratio of 1:1:3 corresponding to the stoichiometric composition of LaFeO_3 .

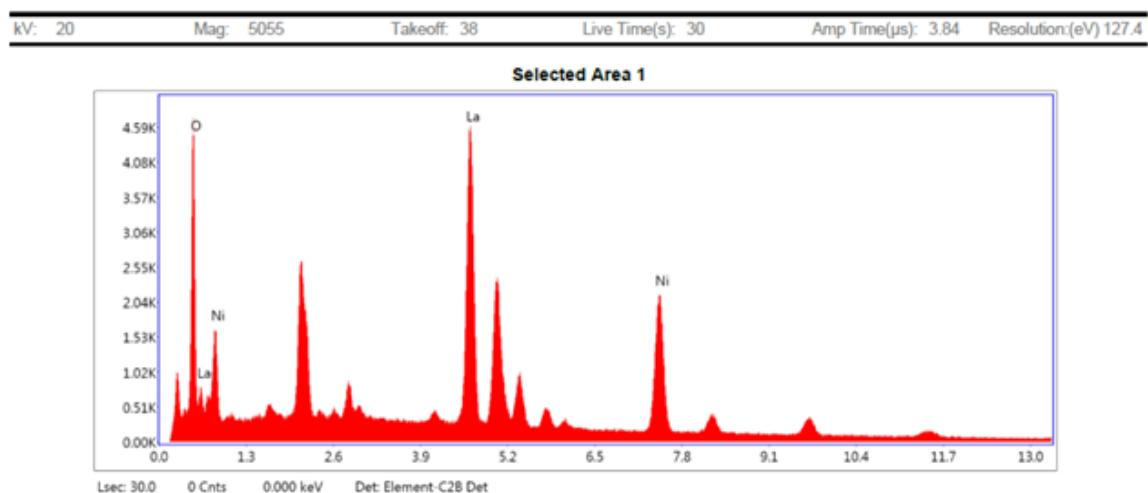


Fig. 7. EDX spectra for LFO nanoparticles.

IV. CONCLUSION

In summary, the synthesis, characterization, composition and band gap energy were studied using a simple technique of preparation at a low temperature of 600°C. Nanosized LaFeO₃ powders of 33.7 nm particle size were prepared directly through the simple sol-gel auto-combustion technique. The entire process of synthesizing pure nanosized LaFeO₃ powders involved three steps: formation of solutions, formation of the dried gel in air followed by auto-combustion that can be considered as a heated-induced exothermic oxidation-reduction reaction between the nitrate and carboxyl groups. The process is easy, simple and cost effective although analytical grade compounds were used as starting materials. The XRD pattern confirmed the formation of a pure LFO phase with a well-defined orthorhombic structure in the space group Pnma, without any impurity phase. The crystalline size of the LFO sample was calculated by the X-ray line broadening method using the Scherrer's formula and average crystalline size is calculated to be about 33.7 nm. FTIR measurements performed on the powders indicate a clear existence of the Fe-O stretching and the bending vibration mode, and the peaks reveal a characteristic of the octahedral FeO₆ groups in the perovskite compound and existence of the LFO phase. UV measurements performed on the powders reveal band gap energy of about 1.7 eV. SEM measurements indicate particles with an average size of 31.2 nm, which is consistent with the size obtained from the peak broadening in X-ray diffraction studied of LFO. Such a consistency implies that the LFO nanoparticles are single crystalline. EDX measurements performed on the powders is a clear confirmation of the existence of La, Fe and O elements.

ACKNOWLEDGMENTS

The authors wish to thank Prof. K.R. Priolkar for help extended in carrying out UV measurements at the Department of Physics, Goa University, India, USIC, Goa University, India, for SEM and EDX measurements, St. Xavier's College of Arts, Science and Commerce, Goa, India for XRD measurements, Mr. Vishnu Chari, Dhempe College of Arts and Science for help in sample preparation. This work was done with no funding from any agency and carried out as a requirement of project dissertation by the authors.

REFERENCES

- [1]. Nguyen Q. Minh, J. Am. Ceram. Soc. 76(4) (1993) 563-588.
- [2]. A. Demastro, Daniele Mazza, S. Ponchetti, M. Vallino, Mater. Sci. Eng. B-Solid 79(2) (2001) 1401-145.
- [3]. G. Martinelli, M.C. Carotta, M. Ferroni, Y. Sadaoka, E. Traverse, B-Chem. 55(2-3) (1999) 99-110.
- [4]. C. Vazquez, P. Kogerier, M.A. Lopez-Quintela, R.D. Sanchez, J. Mater Res. 13(1) (1998) 451-456.
- [5]. J. Xiao, G.Y. Hong, D.C. Yu et al, Acta. Chim. Sinica 52(8) (1994) 784-788.
- [6]. S.S. Manoharam, K.C. Patil, J. Solid State Chem. 102(3) (1999) 267-276.
- [7]. H.B. Park, H.J. Kweon, Y.S. Hong et al, J. Mater. Sci. 32(1) (1997) 57-65.
- [8]. Z.X. Yue, J. Zhou, L.T. Li et al, J. Magn. Magn. Mater. 208 (1) (2000) 55-60.
- [9]. W. J. Zheng, R.H. Liu, D.K. Peng et al, Mater. Lett. 43 (1-2) (2000) 19-22.
- [10]. Xiwei Qi, Ji Zhou, Zhenxing Yue, Zhilun Gui, Longtu Li, Ceramics International 29 (2003) 347-349.
- [11]. Yanping Wang, Junwu Zhu, Lili Zhang, Xujie Yang, Lude Lu, Xin Wang, Materials Letters 60 (2006) 1767-1770.
- [12]. F. Zaza, V. Pallozzi, E. Serra and M. Pasquali, NANOFORUM 2014.
- [13]. Y. Zhao et al, Physics of the Earth and Planetary Interiors, 76, 1-16 (1993).
- [14]. Nur Afifah and Rosari Saleh, Journal of Physics: Conference Series 710 (2016) 012030.